ACTA METALLURGICA SLOVACA
2023, VOL. 29, NO. 2, 75-81

RESEARCH PAPER

A COMPARATIVE ANALYSIS AMONG THE WELDED Al-6061 PLATES JOINED BY FSW, MIG AND TIG WELDING METHODS

Aaluri Praveen Reddy[1], *Saurabh Dewangan*[1]*

[1] Department of Mechanical Engineering, Manipal University Jaipur, Jaipur, Rajasthan, India, Pin-303007

*Corresponding author: (Saurabh Dewangan) saurabh22490@gmail.com, tel.: 0141-3999100-838, Manipal University Jaipur, 303007, Jaipur, Rajasthan, India

Received: 14.04.2023
Accepted: 05.06.2023

ABSTRACT

The present work deals with the assessment of tensile strength, hardness, fracture behavior and microstructural changes in welded Al-6061 plates. Based on that, the performance of three different welding techniques- friction stir welding (FSW), metal inert gas welding (MIGW) and tungsten inert gas welding (TIGW) has been compared. MIG welding has been done with a filler rod whereas no filler metal has been applied during TIG welding for comparing the results with FSW, filler-less solid-state welding. The ultimate tensile strength (UTS) of MIGW sample has been found 75% and 111% higher than that of FSW and TIGW samples respectively. Also, the elongation shown by MIG joint is nearly 50% higher than that of the other two welds. The tensile properties of two non-filler welds, i.e., FSW and TIG have been found similar. The fractography results have established the ductile behavior of all three joints. The primary phase (bright Al-grains) of the base metal zone (BM) with thin solid boundary has changed into thick dendritic shapes in the welded zone (WZ). Also, the coarse secondary phase of BM has converted into fine particles in WZ under the influence of rapid cooling. The WZ has been reported harder than HAZ in MIG and FSW plates whereas the HAZ of TIGW plate has been found harder than WZ due to the accumulation of fine equiaxed secondary phase.

Keywords: Al-6061; FSW; MIGW; TIGW; Tensile strength; Fracture behavior; Hardness; Microstructure

INTRODUCTION

Aluminium (Al) is a soft, highly ductile, and less-hard material due to its FCC lattice structure. Its strength is comparatively less than other materials like hardened steel, carbides, and ceramics etc. Al is a highly corrosion resistant metal due to the formation of a thin transparent oxide film on the newly polished surface which acts as a protective layer against atmospheric corrosion. Al and its alloys are utilised in many industries like aerospace, automobiles, food, and agro-industry. Among all, Al-6160 is the most widely used alloy for different general purposes works and kitchen utensils. Mg, Fe, Si are the main alloying elements in 6160. In addition, small amounts of Cu and Mn are also added. The presence of Mg reduces the melting point of Al [1, 2]. The microstructure of aluminium alloy consists of primarily Al-matrix which imparts Al+Fe+Mn compound whereas a secondary phase (Al+Mn) in the form of fine black particles is dispersed throughout the matrix [3]. The orientation of grain boundaries changes according to variation of heating and cooling rate.

Aluminium is difficult to weld metal by any of the arc welding techniques. Due to its low melting temperature, a less heat input is required at the fusion zone. TIG and MIG welding methods may be applied to weld aluminium plates. TIG provides a clean welding due to less heat input and thereby no splashing of molten metal. It was investigated in a study that hardness of 6082 alloy was higher at low current, and it had reduced with increasing current [4]. It was observed that the microstructure was coarse and globular at high heat input values [5]. The application of filler metal was analysed on the welding process of 6061 Al alloy. The joint was made by TIG welding. The filler ER-4043 showed higher hardness than ER-4047 [6]. In a study with 5083-alloy, it was seen that tensile strength of the joint increased with an increase in welding speed. But, after a certain value, a decrement was also noted in the same [7].

Regarding MIG welding, not much research work has been conducted earlier. In a work, MIG welding between 6061 and 7075 alloy was done. The mechanical characteristics and microstructural attributes of the joint were analysed. The weldment hardness was found higher in 6061 alloy. The tensile strength of the similar joint was reported higher than that of the dissimilar joint. The intermetallic formation in the welded zone was responsible for the high strength of the joint [8].

The problems during melting and solidification of metal in arc welding can be avoided by using solid-state welding like friction stir welding. Al-6061 has been widely used under FSW for studying various parameters like strength, hardness, toughness, and microstructural attributes. The use of FSW technology in joining dissimilar aluminium alloys like AA6061-T6 and AA7075-T6 has allowed for the exploration of cheaper materials. A study investigated the microstructural and mechanical properties of 20 joints created by adjusting parameters such as tool rotating speed, welding speed, axial load, and tool shoulder to pin diameter ratio. Each joint was analyzed for macro-, microstructural-, and fractographic features, with a focus on tensile strength, hardness, and grain size variations. The failure mode was identified as a ductile fracture. The results showed that the best welds were produced at rotating speeds of 1100 RPM, welding speeds of 26 mm/min, axial loads of 7 kN, and tool shoulder to pin diameter ratios of 3, resulting in improved mechanical behavior due to a decrease in particle size in the stir zone [9]. Another work explores the use of FSW technology in joining different types of aluminium alloys, namely AA6061-T6 and AA7075-T6, to make production more cost-effective. The researchers examined the microstructural and mechanical properties of 20 joints made

by adjusting several parameters, such as tool rotating speed, welding speed, axial load, and tool shoulder to pin diameter ratio. They analyzed each joint for macro-, microstructural-, and fractographic characteristics, focusing on tensile strength, hardness, and grain size changes. The failure mode was identified as a ductile fracture. The results revealed that the optimal welds were achieved with rotating speeds of 1100 RPM, welding speeds of 26 mm/min, axial loads of 7 kN, and tool shoulder to pin diameter ratios of 3. The improved mechanical behavior was attributed to a reduction in particle size in the stir zone [10]. In a work, the purpose was to examine how welding speed and the shoulder diameter to pin diameter ratio (D/d ratio) impact the microstructure and mechanical properties of dissimilar AA2014-T6 and AA7075-T6 aluminum alloy butt joints made using friction stir welding. Six joints were created using different D/d ratios and welding speeds, while the tool rotational speed and axial load were kept constant. The study found that the D/d ratio significantly affected the mechanical properties of the joints, which had distinct microstructures with various zones formed by plastic deformation and recrystallization during welding. X-ray diffraction analysis was used to predict the formation of precipitates that affect joint properties. The research also discussed fractographic images of joints created with a D/d ratio of 3, a tool rotational speed of 1200 RPM, a welding speed of 20 mm/min, and an axial load of 8 kN. These joints exhibited higher tensile strength and hardness [11]. Al5086 has been tried to join with steel IS2062 by using filler rod of ER5356. With a proper set of voltage and current, a satisfactory result has been found [12]. After analyzing the friction stir welded joints of Al6160-T6, it has been established that it is the welding speed which predominantly affects the weld quality of joint. As soon as the speed is increased, better stirring occurs which confirms the high-quality bonding [13]. In a work, 2219-Al alloy has been welded by using the high frequency pulsed MIG method. As a result, significant refinement of weld grains has been reported. Hence, a high reduction of pores and low segregation of Cu at the weld area have been reported in the study [14]. It has been seen that porosity and crystallization development are the two unavoidable problems during TIG welding of Al-alloys. High heat input is the suggested method to avoid porosity formation during welding [15].

In this way, there are several works on joint analysis of welded Al-plates. In this direction, the present works explains a comparative assessment of weldability of Al-6061 plate by applying three different welding techniques named TIG, MIG and FSW. The detailed experimental work and result analysis have been provided in the below sections.

MATERIAL AND METHODS

Six aluminium plates of 6061 grade were collected. Each plate has a dimension of 100×50×4 mm. Three pairs were made from these six plates. The first pair was joined by friction stir welding. The FSW tool was made of D2 die steel with a cylindrical probe projected over the shoulder. The height of the probe is 5 mm. The tool rotational speed was 900 RPM and welding speed was 25 mm/min. Another pair was welded through metal inert gas welding (MIG) with current and voltage selection of 153 A and 21 V respectively. The welding speed was 7 m/min in this case. The third pair was welded by tungsten inert gas welding (TIG). The yield parameters selected for this joint were 150 A and 21 V. The welding speed was kept the same as in MIG. TIG welding was performed without using filler metal whereas MIG welding was done with a filler rod of ER5183 which contains Si (0.4%), Fe (0.25%), Cu (0.98%), Mn (0.6%), Mg (4.9%), Cr (0.2%), Zn (0.21%), Ti (0.11%) and Al (Remaining). The shielding gas of Ar-99% purity has been supplied during both arc welding phenomena. The welding methods and three welded plates are shown in **Fig. 1**.

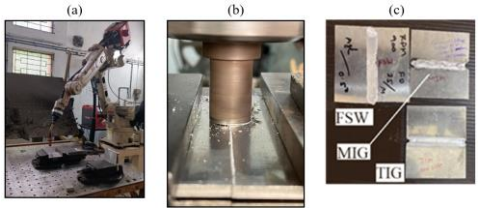

Fig. 1 Experimental work: (a) Automatic MIG welding; (b) FSW process; (c) Three welded plates

After welding, all three plates were fixed on wire-electric discharge machining (WEDM) set up for preparing the tensile test specimens as per ASTM-E8 standard. The WEDM process and tensile test specimens are shown in **Fig. 2**.

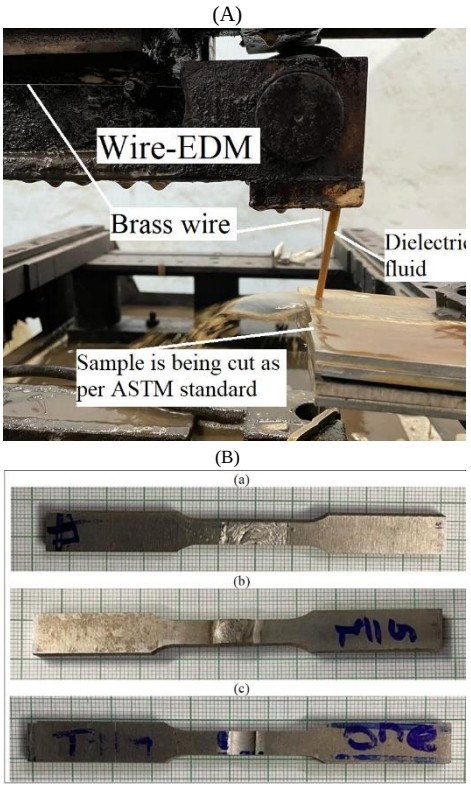

Fig. 2 (A) Cutting of tensile test specimen according to ASTM-E8 standard; (B) Three tensile test specimens of- (a) FSW plate; (b) MIGW plate; (c) TIGW plate

Other plates of 10 mm width were cut from each plate across the welded joint. These plates of 100×10×4 mm dimension were used for hardness test, at one cross sectional area, and for the

microstructural test, for another cross-sectional area. For hardness test, Rockwell hardness tester with B-scale was considered in this work. The hardness testing procedure and used samples are shown in **Fig. 3**.

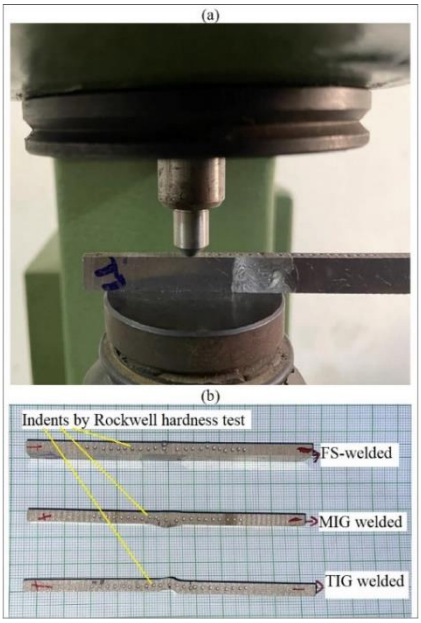

Fig. 3 Rockwell hardness testing: (a) Image during indentation at a gap of 2 mm; (b) The tested specimens

RESULTS

Tensile test: The tensile tests have been performed on FIE Make Universal Testing Machine, UTES 40. The results have been received in the form of Load-displacement graphs for each sample. **Fig. 4** is showing three such graphs. Black colored curve belongs to FSW plate in which YS and UTS are noted as 76 MPa and 88 MPa respectively. The UTS was observed at a maximum load of 2 kN. After reaching up to UTS, a sudden drop in load was observed due to necking. The strain hardening phenomenon after a sudden drop of load has again increased the deformation load till 1.5 kN. Then, the material starts to flow till fracture. A total elongation of 1.6% has been observed in FSW sample.

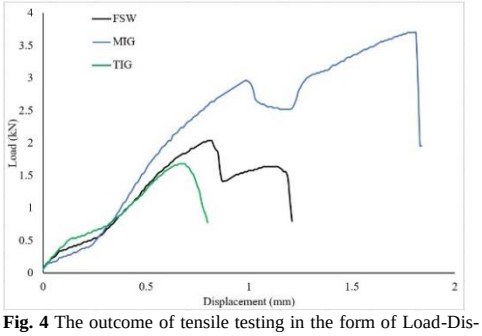

Fig. 4 The outcome of tensile testing in the form of Load-Displacement curves: (a) Blue colored curve- MIGW; (b) Black colored curve- FSW; (c) Green colored curve- TIGW

The pattern of the load-displacement curve of MIG welded sample is almost the same as FSW except for the presence of high strain value during yielding phenomenon (blue colored curve in **Fig. 4**). After a load value of 3 kN, a high yielding and good strain rate was observed in the sample. The strain hardening phenomenon has improved the deformation load value to 3.7 kN. The UTS, YS and elongation shown by this sample are far better than these of FSW sample. The UTS (154 MPa) and YS (123 MPa) of MIG joint are nearly 75% and 62% higher than the same parameters of FSW joint. Also, the elongation received by the sample is 50% greater in MIG joint. These data prove that the MIG joint is stronger and better than FSW.

As compared to the above two joints, TIG weld has not shown a decrement in load and considerable yielding during the test, although the elongation of this joint is comparable with FSW. The yielding was observed at 1.5 kN in this sample. The UTS and YS of the joint are 73 MPa and 65 MPa respectively. As compared to FSW and MIG, the UTS of TIG joint is respectively 17% and 53% lower (Green colored curve in **Fig. 4**). As the TIG welding was performed without filler metal, the strength has negatively affected. As far as filler-less welding is concerned, the observations of TIG welding prove that FSW can be a better option in terms of high strength and ductility. All the main observations recorded by tensile tests of three plates are written in **Table 1**.

Table 1 Observations recorded from tensile test

Sample	Tensile strength (UTS) MPa	Yield stress (YS) MPa	% Elongation
FSW welded	88	76	1.6
MIG welded	154	123	2.4
TIG welded	73	65	1.7

Fractography analysis: All the welded plates have fractured from welded joint. The fractured tensile specimens, as shown in **Fig. 5**, have been taken into fractography analysis under FESEM machine. For performing this test, the small part of fractured region has been cut-off from the sample and the central part of the fractured area has been taken into microscopic observation.

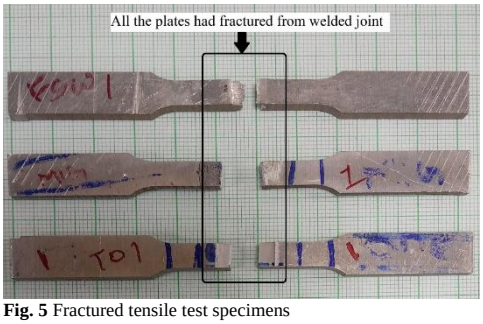

Fig. 5 Fractured tensile test specimens

The fractographic images are shown in **Fig. 6**. All the images were captured at the scale of 20µm and 500X magnification. **Fig. 6(a)** is the fractographic image of FSW sample which contain a little amount of plastic flow of material, yet the presence of macro- and micro-dimples is almost negligible in the captured image. A mixed behavior of good yielding and less elongation could be seen in the FSW sample. **Fig. 6(b)** belongs to MIG welded specimen. Considerable plastic deformation in the form

of layer-wise material flow could be seen in the image. Also, macro-dimples as the result of valley formation due to cup-cone fracture are responsible for high elongation rate and high yielding during tensile test. Fig. 6(c) is showing the image of TIG welded joint. The fractured surface image and parameters obtained through tensile test do not justify each other. In the fractographic image, a good whirl-like appearance proves a good elongation while the sign of plastic flow is an indication of good ductility. There is a high possibility of defects inclusion during TIG welded joint.

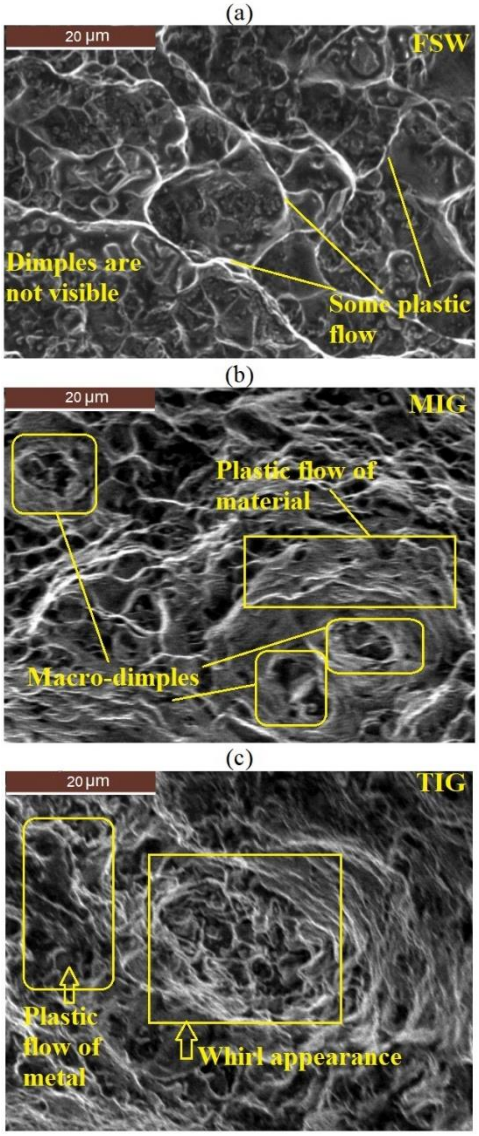

Fig. 6 Fractography analysis of welded joint: (a) FSW joint; (b) MIG joint; (c) TIG joint

Hardness test analysis: The Rockwell hardness-B scale test was performed on the finished cross-sectional area of each welded plate. Initial indentation was done on the weld-center position. Besides this, 10 indentations were made at a common gap of 2mm on each side (right and left) of the welded joint. Considering the weld center position as '0', the leftward positions were indicated by negative sign whereas the rightward was positive. The hardness values obtained through each indentation on each plate were plotted in the form of a comparative graph (**Fig. 7**). As per the graph, the BM possesses the highest hardness. As soon as the indentation is moved towards HAZ, a decrement in hardness was recorded. The WZ of MIG and FSW joints has been seen as harder than HAZ. In TIG joint, the HAZ was observed as harder than WZ. The hardness profile of MIG and FSW welded plates is similar in nature. For better understanding, a comparative bar chart of hardness among different zones of the plates has been presented in **Fig. 8**. In all the zones, the MIG welded plate has shown the highest hardness, whereas the TIG welded plate is the least hard sample in this study.

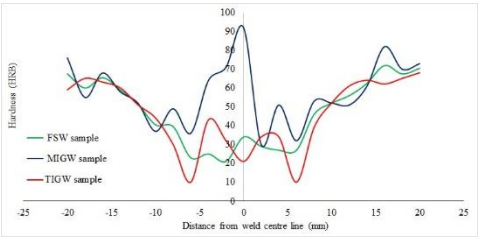

Fig. 7 Hardness distribution at various points of the welded plates

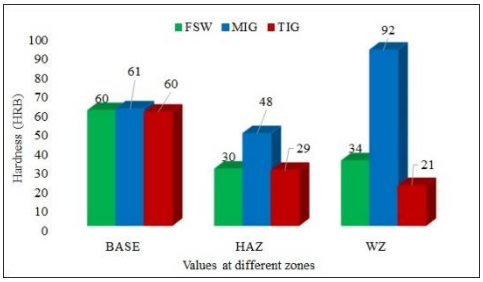

Fig. 8 A comparative assessment among hardness at BM, HAZ and WZ

MICROSTRUCTURAL ANALYSIS

It is a difficult task to polish the aluminium alloy to give it a mirror-finish because it forms a very thin layer of oxide which protects it from further atmospheric oxidation. The cross-sectional surfaces of all the welded plates were properly polished by using all the necessary steps involving sandpaper finishing and rubbing against the high-speed polisher with fine abrasive particles. Fine-grained polishing papers (of grade 2800, 3000, and 3200) were used under study. The etchant of 2% hydrofluoric acid (HF) was prepared for application on the polished surface of the samples. The etchant was applied for approximately 3 min. The polished and etched surfaces of the three plates are shown in **Fig. 9**.

The grain size orientation in FSW plate is fine and equiaxed. Both bright and black colored phases which are termed as primary and secondary phases of Al are globular in size. In the thermo-mechanical affected zone, no boundary between BM and WZ (stirred zone) has been observed. The grain appearance in WZ is finer than BM. A similar appearance of BM and WZ establishes that friction stirring has been done properly (**Fig. 10**).

The BM of MIG welded plate can be seen with black colored solidified grain boundary of primary Al-grain. The primary phase of Al is completely bright in appearance. The black spots are Al-Mn based secondary phase. As soon as the observation approaches HAZ, the thin solidified boundaries get converted into thick dendrites. The fusion of thin and thick grain boundaries has resulted in a lesser hardness of the HAZ. According to previous studies, the normal rate of solidification enhances the formation of dendritic Al until the beginning of nucleation of Al6Mn. The slow cooling process delays the formation of Al-Fe-Si-Mn particles. However, the way of dendritic growth of primary-Al and secondary (Al6Mn) is competitive in nature. It has been observed that the size of Al6Mn dendrites may reduce because of rapid cooling [16, 17]. In this work, the WZ was cooled rapidly under atmospheric air. Due to this, grain boundaries are thick and the secondary phase is too fine, as shown inside the yellow rectangular area in **Fig. 11**.

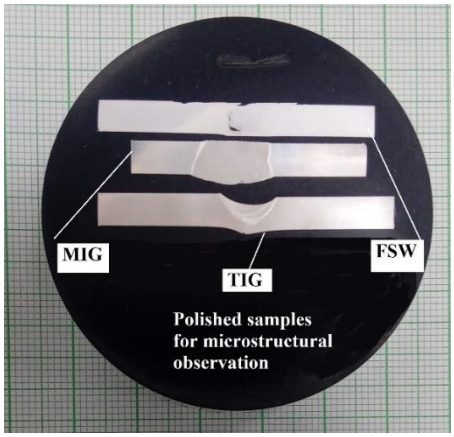

Fig. 9 Polished and etched surfaces of three welded plates

Fig. 12 is showing the microstructural images of TIG welded plate. The BM is possessing thin solidified rain boundaries of primary Al-phase. Both coarse and fine sized secondary phase have been seen in the image. Fig 12(b) is showing a wide HAZ between BM and WZ. Unlike MIG welded joint, the HAZ of TIG involves accumulation of fine and globular secondary phase which is the main cause of high hardness of HAZ than WZ. As shown in Fig. 12(c), the appearance of WZ is very similar to that of MIG. The dendritic and thick grain boundary with fine secondary phases is reported in the WZ of TIG.

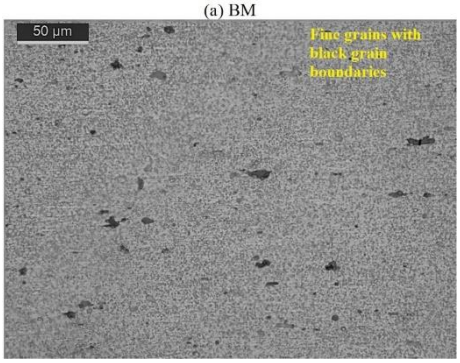

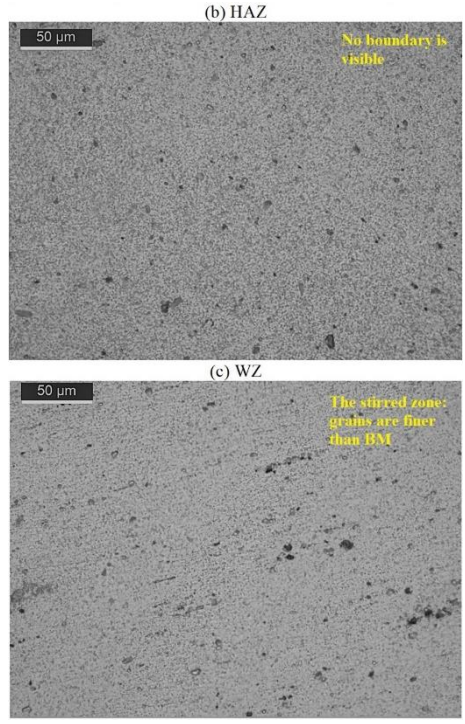

Fig. 10 Microstructural observation in FSW plate

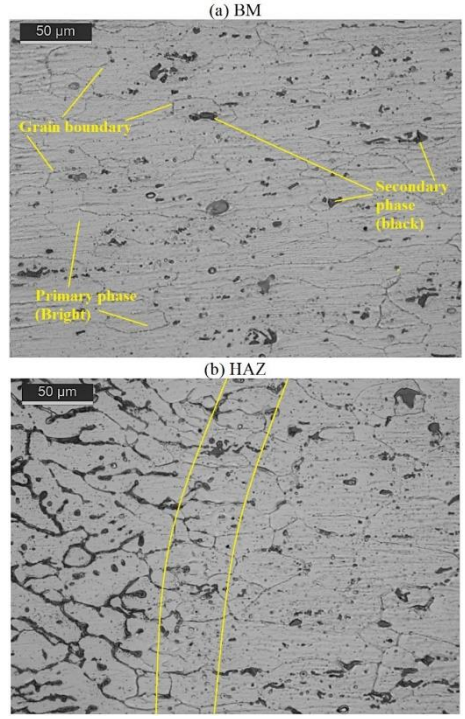

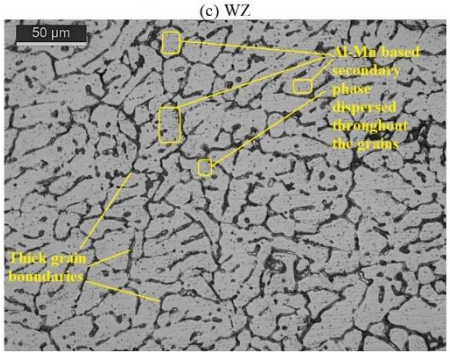

Fig. 11 Microstructural observation in MIGW plate

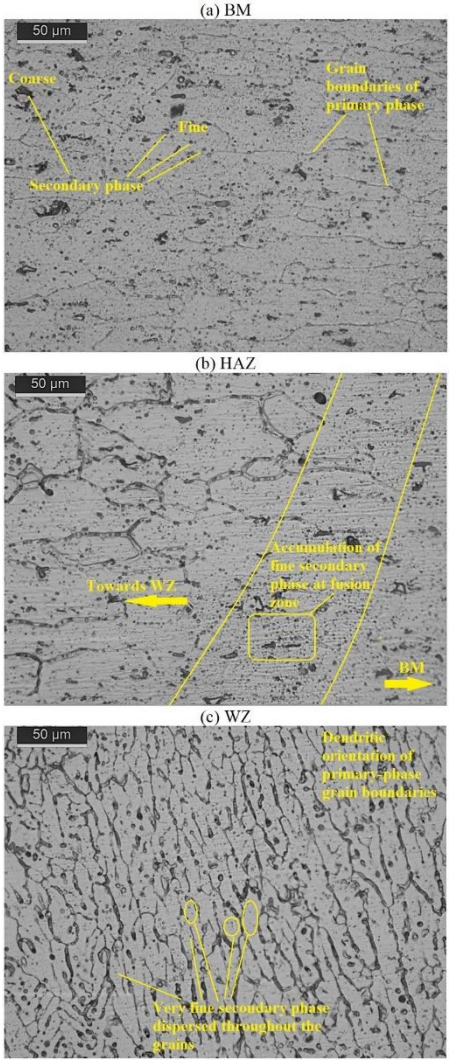

Fig. 12 Microstructural observation in TIGW plate

CONCLUSIONS

Al-6061 possesses good weldability under both types of welding conditions i.e., solid state and liquid state. In this work, an attempt has been made to compare and analyze the mechanical properties and microstructural changes in Al-6061 plates after three different welding- FSW, MIG and TIG. These three weldings are commonly applied in Al-alloys. As per the results obtained by tensile, hardness, fractography and microstructural tests, the following conclusions can be drawn from this study:

- The MIGW plate, in which filler was used, has shown the highest values of UTS (154 MPa) and YS (123 MPa) with 2.4% of elongation. FSW, a filler-less solid-state welding process, has shown UTS of 88 MPa which is 43% lower than that of MIGW sample, although the elongation (1.6%) is satisfactory. The lowest value of UTS (i.e., 73 MPa) was recorded in filler less and single side TIG welded plates. The elongation of 1.7% in TIG plate is comparable to FSW. It proves that insertion of filler wire is highly necessary in the case of arc welding.
- Although the FSW plate imparts better UTS than TIGW plate, the ductile properties of the WZ have lost in FSW plate due to improper stirring. Hence, it's important to provide enough speed to the tool so that adequate mixing of the adjoining edges can be done.
- Both the arc welded joints have shown a ductile behavior of the fracture by possessing a considerable plastic flow. Also, both, macro- and micro-dimples have been reported in the fractured region whereas the FSW does not contain any dimples except a little amount of plastically deformed zone.
- Hardness results establish that WZ of MIGW sample is significantly higher by 170% and 338% than that of FSW and TIGW samples respectively. The HAZs in FSW and MIGW samples have been reported as less hard than other zones of the plates whereas, in TIGW sample, the accumulation of secondary phase has made the HAZ comparatively harder than BM and WZ.
- As per the microstructural observation, the fine solid grain boundaries of primary phase in BM get converted into thick dendrites in WZ. Also, the coarse secondary phase (black) of BM has changed into fine particles in the WZ. The negligible appearance of BM-WZ boundary in FSW plate has established the occurrence of proper mixing of metal due to stirring.
- MIG welding with filler wire has been proven as the highly suitable method for joining Al-plates as far as good strength, high ductility, and high hardness is concerned.

REFERENCES

1. O. Yakubu, I. Usman, A. Aliyu, O.O. Emmanuel: Nigerian Journal of Technology, 35(1), 2015, 122-128. https://doi.org/10.4314/njt.v35i1.19.

2. A.M. Samuel, F.H. Samuel, C. Villeneuve, H.W. Doty, S. Valtierra: International Journal of Cast Metals Research, 14, 2001, 97–120. https://doi.org/10.1080/13640461.2001.11819429.

3. I. Polmear, D. St John, J.-F. Nie, M. Qian. Chapter 1: The Light Metals. In.: *Light Alloys: From Traditional Alloys to Nanocrystals*. Fifth Edition, Butterworth-Heinemann: Oxford, 2017, 1-29. https://doi.org/10.1016/B978-0-08-099431-4.00001-4.

4. A. Laska, M. Szkodo, D. Koszelow, P. Cavaliere: Metals, 12, 2022, 192. https://doi.org/10.3390/met12020192.

5. F. Gulshan, Q. Ahsan: Chemical and Materials Engineering, 2, 2014, 25- 32.
6. M. Samiuddin, J. Li, M. Taimoor, M. N. Siddiqui, S. U. Siddiqui, J. Xiong: Defence Technology, 17, 2021, 1234-1248. https://doi.org/10.1016/j.dt.2020.06.012.
7. M. Dorta-Almenara, M. C. Capace: Revista Facultad de Ingeniería, 25, 2016, 7–19. https://doi.org/10.19053/01211129.v25.n43.2016.5293.
8. I. Sevim, F. Hayat, Y. Kaya, N. Kahraman, S. Sahin: The International Journal of Advanced Manufacturing Technology, 66, 2013, 1825–1834. https://doi.org/10.1007/s00170-012-4462-z.
9. V. Saravanan, S. Rajakumar, A. Muruganandam: Metallography, Microstructure and Analysis, 5, 2016, 476–485. https://doi.org/10.1007/s13632-016-0315-8.
10. P. Carlone, G. S. Palazzo: Metallography, Microstructure and Analysis, 2, 2013, 213–222. https://doi.org/10.1007/s13632-013-0078-4.
11. V. Saravanan, N. Banerjee, R. Amuthakkannan, S. Rajakumar: Metallography, Microstructure and Analysis, 4, 2015, 178–187. https://doi.org/10.1007/s13632-015-0199-z.
12. R. Sachin, A. Sumesh, U.S. Upas: Materials Today: Proceedings, 24, 2020, 1167-1173. https://doi.org/10.1016/j.matpr.2020.04.430.
13. S. Dewangan, R. Yadav, A. Sharma, S. Vohra: Advances in Processing of Lightweight Metal Alloys and Composites. In: Vignesh, R.V., Padmanaban, R., Govindaraju, M. (eds) *Advances in Processing of Lightweight Metal Alloys and Composites*. Materials Horizons: From Nature to Nanomaterials. Springer: Singapore, 2023, 281-298. https://doi.org/10.1007/978-981-19-7146-4_16.
14. X. Kuang, B. Qi, H. Zheng: Journal of Materials Research and Technology, 20, 2022, 3391-3407. https://doi.org/10.1016/j.jmrt.2022.08.094.
15. V. Manikandan, K. Mariselvam, R. Nekin Joshua, C. Ramesh, K. Arunprasath: Materials Today: Proceedings, 66, 2022, 683-689. https://doi.org/10.1016/j.matpr.2022.03.641.
16. D.T.L. Alexander, A.L. Greer: Acta Materialia, 50, 2002, 2571–2583. https://doi.org/10.1016/S1359-6454(02)00085-X.
17. I. Polmear, D. St John, J.-F. Nie, M. Qian. *Light Alloys: Metallurgy of the Light Metals*. Butterworth-Heinemann: Oxford, 2017, 31-107. https://doi.org/10.1016/B978-0-08-099431-4.00002-6.